Scan to know paper details and author's profile

Reliability of the Bond Graph Approach for Robust Diagnosis of a Newborn Incubator System

Abderrahmene Sellami, Zermani Mohamed Aymen, Elyes. Feki & Abdelkarim. Mami

Université de Tunis

ABSTRACT

This article aims to solve a problem of research with a thermal system (incubator) to the graph of pseudo-connections. The method we develop is based on the determination of the resolution on the model ARR-BGM (Analytical Redundant Relationships Bond Graph). These relationships serve to detect and isolate faults in the various elements of the system, but also to locate the industrial system. We introduced defects in the heat source, leaks in the incubators and a leak in the incubator door; these defects were transferred by thermal transfer to negative values. The results of simulation, the effectiveness of proposed method to detect and locate defects, in addition, to analyze the robustness of the Incubator to defects, we imported the graphical link model as linear fractional transformations (BG-LFT). This makes it possible to verify the reliability of the approach of the link graphs in terms of sensitivity and detectability of defects that may appear in an industrial system.

Keywords: robust diagnosis, bond graph approach, linear fractional transformations, analytical redundancy relations, incubator.

Classification: LCC Code: T58.5

Language: English

Great Britain Journals Press

LJP Copyright ID: 392924
Print ISSN: 2631-8474
Online ISSN: 2631-8482

London Journal of Engineering Research

Volume 24 | Issue 1 | Compilation 1.0

Reliability of the Bond Graph Approach for Robust Diagnosis of a Newborn Incubator System

Abderrahmene Sellami[α], Zermani Mohamed Aymen[σ], Elyes. Feki[ρ] & Abdelkarim. Mami[Ѡ]

ABSTRACT

This article aims to solve a problem of research with a thermal system (incubator) to the graph of pseudo-connections. The method we develop is based on the determination of the resolution on the model ARR-BGM (Analytical Redundant Relationships Bond Graph). These relationships serve to detect and isolate faults in the various elements of the system, but also to locate the industrial system. We introduced defects in the heat source, leaks in the incubators and a leak in the incubator door; these defects were transferred by thermal transfer to negative values. The results of simulation, the effectiveness of proposed method to detect and locate defects, in addition, to analyze the robustness of the Incubator to defects, we imported the graphical link model as linear fractional transformations (BG-LFT). This makes it possible to verify the reliability of the approach of the link graphs in terms of sensitivity and detectability of defects that may appear in an industrial system.

Keywords: robust diagnosis, bond graph approach, linear fractional transformations, analytical redundancy relations, incubator.

Author α: Laboratoire d'Application de l'Efficacité Énergétique et des Énergies Renouvelables-LAPER, Faculté des Sciences de Tunis, Université de Tunis El Manar Campus Universitaire Farhat Hached, 1068 Tunis, Tunisie.

σ: Laboratoire d'Application de l'Efficacité Énergétique et des Énergies Renouvelables-LAPER, Faculté des Sciences de Tunis, Université de Tunis El Manar Campus Universitaire Farhat Hached, 1068 Tunis, Tunisie.

ρ: Laboratoire d'Application de l'Efficacité Énergétique et des Énergies Renouvelables-LAPER, Faculté des Sciences de Tunis, Université de Tunis El Manar Campus Universitaire Farhat Hached, 1068 Tunis, Tunisie.

Ѡ: Laboratoire d'application de l'efficacité énergétique et des énergies renouvelables, Faculté des Sciences de Tunis University of Tunis el Manar Campus Universitaire El Manar, 2092 Tunis, Tunisia.

I. INTRODUCTION

The main objective of the automation engineer is to determine control algorithms of physical systems that are often of different natures, electrical, mechanical, hydraulic, thermal, etc. This objective will not be obtained if the system modeling is not validated which is the first task. The model describing physical reality is usually obtained on the basis of an idealized description of the system and only dominant phenomena are often taken into account given the complexity and diversification of the system [1-4].

In this article we chose the incubator not only for the complexity of the system but also the importance of this system in the lives of human beings. An incubator is a protected heated place, which allows the development and monitoring of certain newborns. It is an apparatus intended to allow the normal development of children born before term (premature), or fragile newborns [5-10].

The incubators consist of an electrical part (electrical heating resistance) and a thermal part (enclosure receiving the child). Several elements of the incubator can be a source of contamination of the environment of the newborn. Indeed, each part constituting the incubator has specificities for cleaning, disinfection and maintenance. In addition, disinfection is a priority of neonatology

London Journal of Engineering Research

units [11], but maintenance (sealing problem, problem of thermal insufficiency or overheating) is a task for technicians [12-15]. To facilitate the task of the technicians, it is necessary to find a reliable and generous approach to model and analyze the defects that may appear during operation this incubator. This reliability and generosity can be found in several approaches such as Petri nets [16-24] and bond graph [25-30].

Most authors have limited their research to a mathematical model to simulate the different heat exchanges in the incubator or for control purposes..: Ultman [31] developed a simulator of neonatal energy transfer to provide a convenient yet precise comparison of sensible heat loss in incubators, Le BIanc [32] described the fundamental equations involved in thermal exchange between infants and their environment. Simon [33] developed a Theoretical Model of Infant Incubator Dynamics. Pauline Décima[34] developed a Mathematical modeling of thermoregulation processes for premature infants in closed convectively heated incubators and for calculating thermo neutrality in closed incubators for premature newborns, Zermani [35] developed a simulation model of infant-incubator system with decoupling predictive controller, Andrés Fraguela [36] Proposed a model of heat exchange and energy balance in premature newborns during the first hours of life in a closed incubator. In addition, a control problem was proposed and solved in order to maintain thermal stability of premature. Stéphane Delanaud [37] proposed a New Software for assessing the impact of humidity on the optimal incubator air temperature.

The bond graph approach is a very effective approach for this kind of system, since it is multidisciplinary and was initially used for modeling physical systems. The usual approach of the users of this approach is to consider the bond graph model as a knowledge model for the simulation of dynamic systems. The idea of using a single representation (the bond graph) for the modeling, analysis and synthesis of control laws by exploiting causality has been developed in this field [38, 40].

Engr Hassan Javed and Asif Mahmood Mughal [41] have developed a flow chart model for an incubator that only takes into account the heating part modeled as heating capacity, then the heat flux in the chamber is modeled as a flux source, but they neglected the thermal capacity of the external environment and the thermal capacity of the mattress. In this paper we propose a new approach of modeling by the bond graph approach of the incubator taking into account the thermal capacities of the environment as well as the mattress.

The purpose of this article is also to design a robust diagnostic system based on a model using a single tool: the link graph. Methodologically, the work consists of automating model generation and failure indicator procedures in the form of fractional linear transformations (LFTs) and interchangeably for integration into the supervisory system. At the industrial level, the results obtained were applied to real installations: incubator.

II. MATHEMATICAL MODEL OF THE INCUBATOR

The incubator can be described as a reaction system consisting of two large dynamic parts: the climate inside the lodge and the heating system. The heat, humidity and oxygen at the thermostat outlet are defined as input variables of the incubator and the climate parameters tested by the newborn are the output variables. The temperature of the box, the temperature of the walls and the windows intended for medical care, the incubator consists of three main parts:

- The ambient air in the lodge
- The mattress;
- The walls.

2.1 Modeling the Thermostat

To model this part of the incubator, consider the following simplifying measures:

- The thermostat is assumed to be homogeneous with constant characteristics such as specific heat
- The temperature distribution is uniform,
- The specific heat C_{pm} is equal to that of the normal air.

The temperature of the air coming from the thermostat can be written as follows:

$$\frac{dT_{ha}}{dt} = \frac{(T_{hai} - T_{ha})}{C.R_{pm}} \quad (1)$$

2.2 The Ambient Air in the Lodge

The ambient air of the incubator box exchanges heat with all the elements of the Child-incubator system mainly by convection, but also by mass transfer during the Breathing and also by evaporation. In our case we consider the incubator without baby. During a period dt, the thermal equilibrium of the ambient air of the box can be determined according to the following equation:

$$\frac{dT_a}{dt} = \frac{Q_{ht} - Q_{acv} - Q_{mat}}{M_a.C_{pa}} \quad (2)$$

Where M_a denotes the air mass in the box and C_{pa} its thermal capacity.

The ambient air of the box gives heat to the walls of the incubator by convection. This energy is determined by the following equation:

$$Q_{acv} = h_{acv}.A_w.(T_a - T_w) \quad (3)$$

Where A_w is the surface of the walls in contact with the air. The convective transfer coefficient h_{acv} depends mainly on the shape of the incubator, the ventilation in the box and the number of Nusselt and Reynold.

The mattress surface of the incubator not occupied by the child also exchanges the energy with the convective ambient air according to the following equation:

$$Q_{mat} = h_{acv}.A_{net}.(T_a - T_m) \quad (4)$$

Where A_{net} is the surface of the mattress in contact with the air.

2. 3 Thermal Balance of the Walls

The walls of the incubator, made of transparent Plexiglas, have six portholes and a window provided for care. The walls consist of a single homogeneous layer thw thickness equal to 6mm and the heat distribution is uniform on the inner surface and external.

The thermal equilibrium during a time dt can be written in the following way:

$$\frac{dT_w}{dt} = \frac{Q_{acv} - Q_{cv0} - Q_{r0}}{M_w.C_{pw}} \quad (5)$$

Where Mw the total mass of plexiglass walls and C_{pw} its thermal capacity.

The inner surface of the incubator wall receives convective heat loss from the ambient air in the incubator Qacv.

On the other hand, the walls of the incubator exchange with the neonatology room of radiation and convection energy. The convective heat transfer is determined by the equation below:

$$Q_{cv0} = h_{cv0}.A_{wt}.(T_w - T_e) \quad (6)$$

The heat transfer by radiation is calculated by the following relation:

$$Q_{r0} = A_{wt}.\delta.\xi_w[(T_w + 273.15)^4 - (T_e + 273.15)^4] \quad (7)$$

2. 4 Mattress Modeling

The mattress of the incubator exchanges heat by conduction of the ambient air and skin conduction. In the case of an empty incubator the thermal equilibrium of the mattress can then be written in the same way next:

$$\frac{dT_m}{dt} = \frac{Q_{mat} - Q_{ic}}{M_m.C_{pm}} \quad (8)$$

Knowing that the two plates of the support that carries the mattress are thin, and the surface of small contact, the transfer of heat by conduction of the mattress to the incubator, Q_{ic}, is not considerable and can be ignored.

III. INDUSTRIAL SYSTEM BY BOND GRAPH MODELS

The bond graph formality was introduced by H. Paynter in 1961 [42] and formalized by Karnopp and Rosenberg in 1975 [43]. The bond graph tool is now used regularly in a few companies, particularly in the automotive industry (PSA, Renault, Ford, Toyota, General Motors, etc.). This method illustrates energy transfers in the system using power bonds. A power link is symbolized by a half arrow, whose orientation indicates the direction of power transfer. Thus, figure 1 shows the power transfer from subsystem S_1 to subsystem S_2 [44-46]. One of the fundamental characteristics of the bond graph formalism is its unifying aspect, whatever the physical domain of application (electrical, mechanical, hydraulic, chemical...). We can visualize energy transfers in multi-domain systems using the generalized variables presented in the next section. The notion of power is described by the following relation:

$$P(t) = \dot{e}(t).f(t) \tag{9}$$

This equation illustrates energy transfers in the system by using power bonds. A power link[4] is symbolized by a half arrow, whose orientation indicates the direction of power transfer. Thus, figure 1 shows the power transfer from subsystem S_1 to subsystem S_2.

Each power link carries two information's simultaneously: the effort and the flow (see figure 1). These are the generalized power variables (their product being the transferred power).

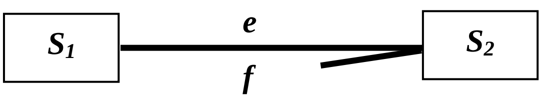

Figure 1: Power link

IV. ROBUST DIAGNOSIS OF INDUSTRIAL SYSTEM BY BOND GRAPH MODELS

Linear Fractional transformations (LFT) are generic objects widely used in the modeling of uncertain systems. The universality of fractional linear transformations is reached seen that any rational expression can be written in this form [47-54]. This form of representation is very used for the synthesis of control laws of uncertain systems using the principle of μ-analysis. It consists of separating the nominal part of a model from its uncertain part, as shown in figure 2.

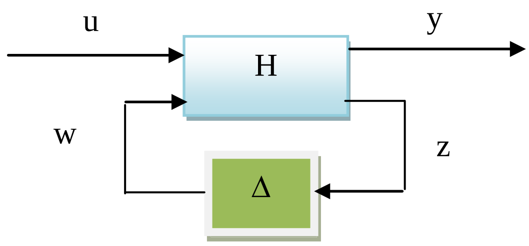

Figure 2: Representation of the Fractional Linear Transformations (LFT)

The nominal values are grouped together in an augmented matrix denoted H, supposed to be proper. The uncertainties whatever their types (structured and unstructured parametric uncertainties, modeling uncertainties, measurement noises, etc.) are combined in a matrix Δ of diagonal structure.

With:

$x \in R^n$: System state vector;
$u \in R^m$: Vector grouping system control inputs;
$y \in R^p$: Vector grouping the measured outputs of the system;
$w \in R^l$ *and* $z \in R^l$: Respectively include inputs and auxiliary outputs. n, m, l and p are positive integers.

4.1. Construction of a BG-LFT Model

All industrial systems can be modeled by BG model according to figure 3. Indeed, the input signal is modeled by an effort source (*Se*) or a flow source (*Sf*). The complete system is modeled by resistive elements (*R*) and storage elements (*I* or *C*), while the detectors are modeled by detector elements (*De* or *Df*).

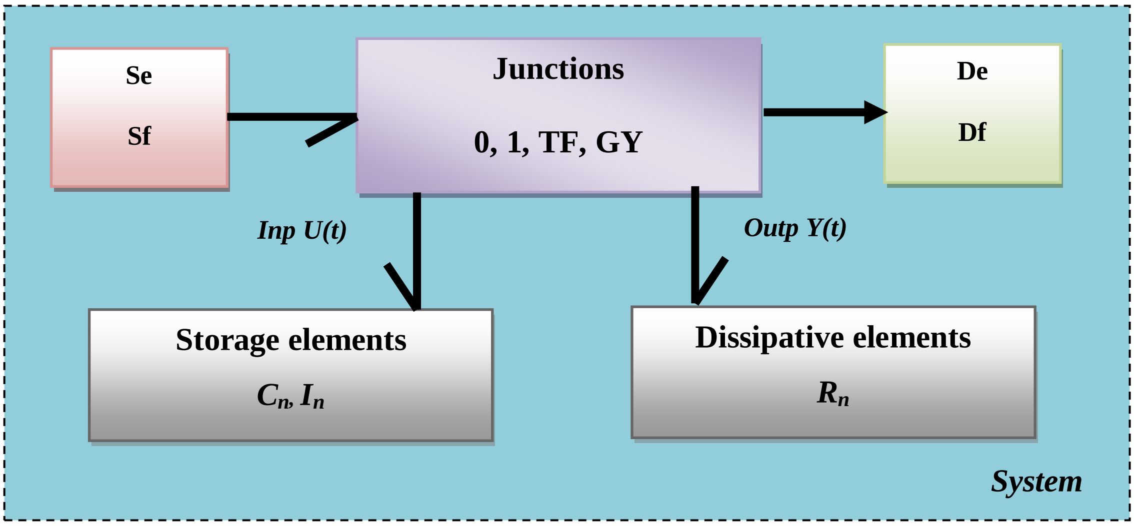

Figure 3: Industrial System Described by Bond Graphs

4.2. Bond Graph Element With Multiplicative Uncertainty

The introduction of a multiplicative uncertainty on e.g. element R in causality gives resistance:

$$e_R = R_n(1+\lambda_R)f_R = e_n + \lambda_R e_n = e_n + e_{inc} \tag{10}$$

With:

- R_n : The nominal value of the element R;
- λ_R: The multiplicative uncertainty parameter;
- e_R et f_R : Represent respectively the effort and the flow in the element R ;
- e_n et e_{inc} : Respectively represent the effort made by the nominal setting and effort introduced by the additive uncertainty.

Unlike the force introduced by an additive uncertainty with respect to the parameter (equation (1)), the force provided by a multiplicative uncertainty (equation (10)) is a function of the force provided by the nominal parameter. This is an important property for the parametric identification step and the supervision step.

4.3 Resistive Element With a Multiplicative Uncertainty

The bond graph model equivalent mathematical model of equation (2) is given in figure 4.

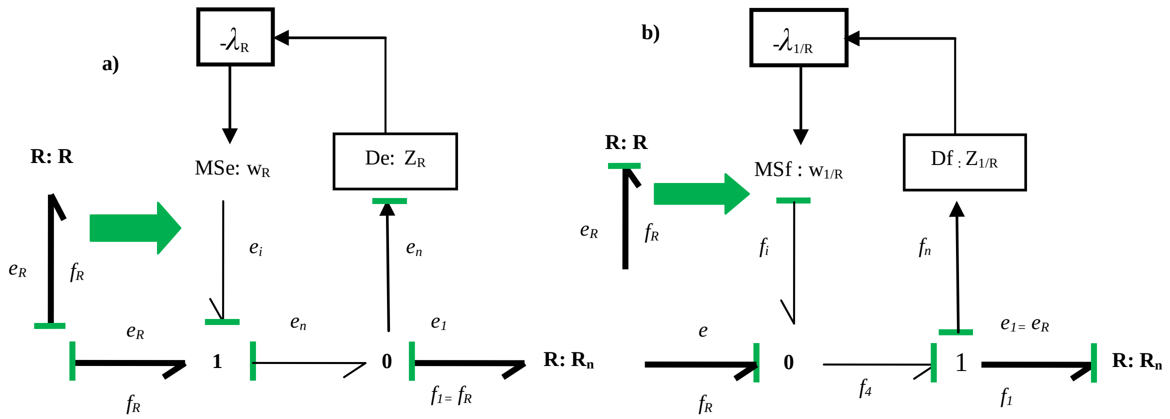

Figure 4: a) BG-LFT Model of an Element Resistance with Multiplicative Uncertainty, b) BG-LFT Model of an Element Conductance with Multiplicative Uncertainty

4.4 Storage Elements With a Multiplicative Uncertainty

- Parts C derived causality

The bond graph model equivalent mathematical model of equation (2) is given in figure 5.

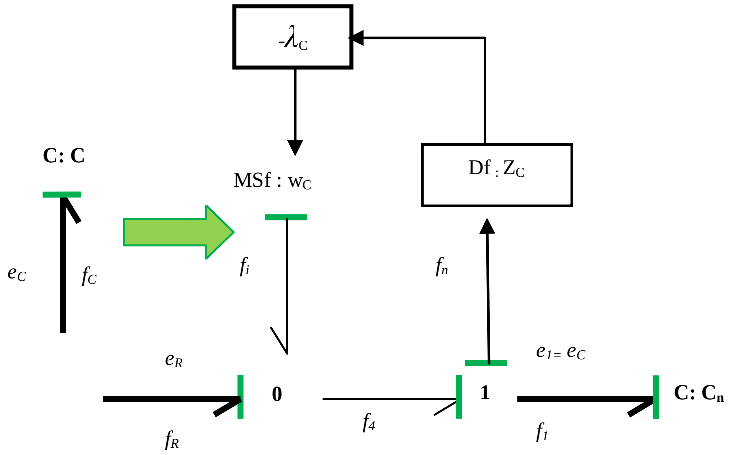

Figure 5: BG-LFT Model of an Element *C* in Derivative Causality With Uncertainty

- Parts C Integral Causality

The bond graph model equivalent mathematical model of equation (2) is given in figure 6.

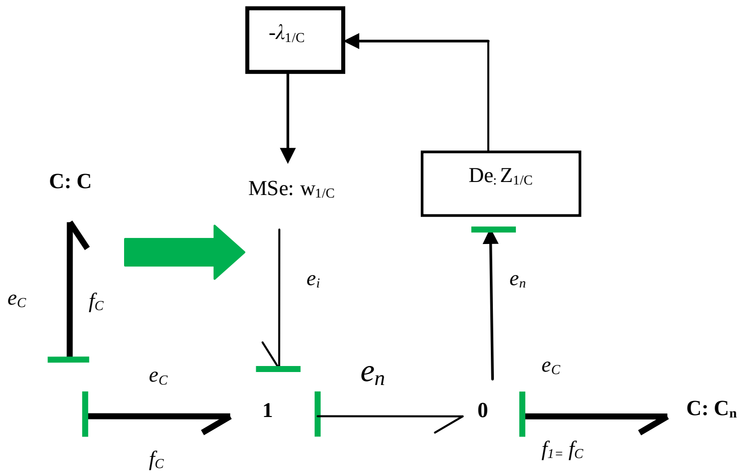

Figure 6: a) BG-LFT Model of an Element C in Integral Causality with Multiplicative Uncertainty

To determine the final model that fits the model of a physical system by the Bond Graph approach and the Linear Fractional transformations model, we must integrate according to the following figure 7.

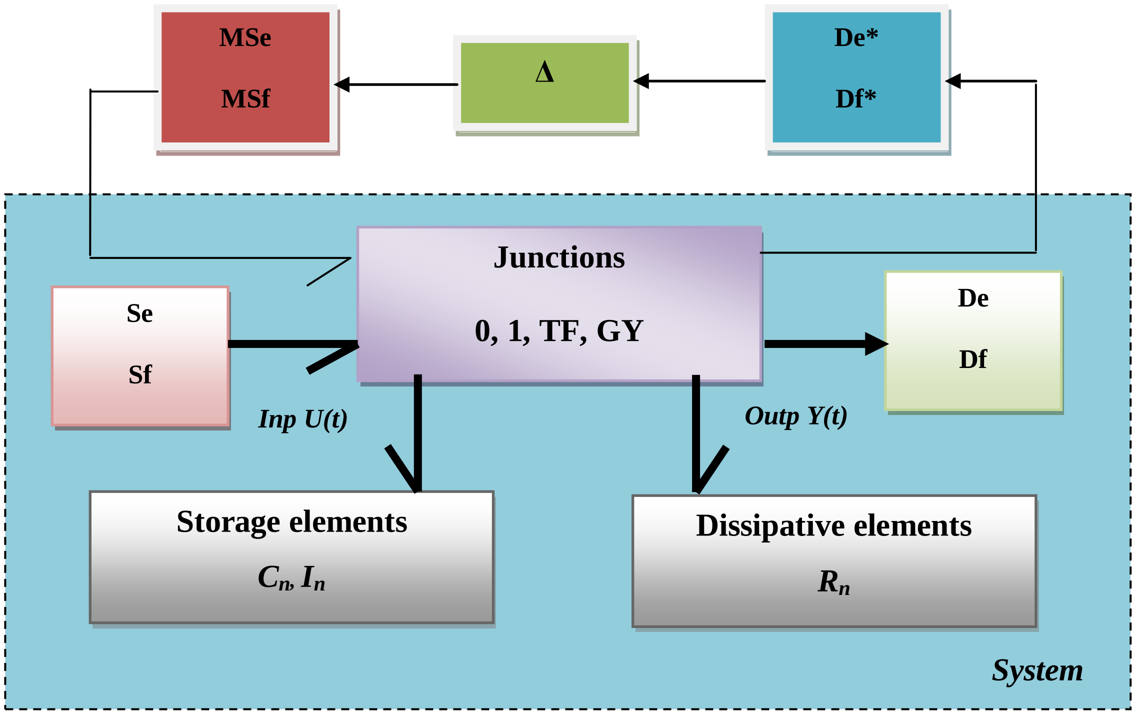

Figure 7: BG-LFT Model for Physical System

4. 5 Generation of Robust Residuals

To determine the residuals by the redundant analytical relationship (*ARR*), the following steps must be followed:

- *1st phase*: Determining the derivative model;
- *2nd phase:* Determining the graph model using the LFT transform;
- *3rd phase:* Determining the residual equations for the two junctions (0 and 1).

For a 0-junction:

$$\sum f_{inc} + \sum Sf + \sum w_i \tag{11}$$

For a 1-junction:

$$\sum e_{inc} + \sum Se + \sum w_i \tag{12}$$

With, e_{inc} and f_{inc} are unknown variables. Moreover, the sum of flow sources and the sum of the effort sources are respectively performed at the level of the 0-junction and the 1-junction. then determine the residue equations at their junctions.

$$ARRs : \Phi(\sum Se, \sum Sf, De, Df, \sum w_i, R_n, I_n, C_n, TF_n, GY_n) \tag{13}$$

where

TF_n and Gy_n are nominal elements *TF* and *GY*.
R_n, C_n, and I_n are nominal elements *R*, *C* and *I*.
$\sum w_i$ are uncertainties on the junction-related items.

V. ANALYSIS OF RESIDUALS SENSITIVITY

The methods of analysis of sensitivity to uncertainties and defects is proposed to improve diagnostic performance has been developed in recent years [68-70]. Indeed, these methods are unfortunately not effective for the generation of residues since they neglect the inter-parametric correlation (the thresholds are often overvalued and may differ). In addition, the Bond Graph tool provides an effective solution to the problem of parametric dependencies since the generation of bond graph using (BG-LFT) automatically separates the residuals and the adaptive thresholds, this separation clearly showing the energy contribution of the uncertainties to the indicators of defects and facilitating their assessments in the decision stage by calculating the adaptive thresholds of normal operation. The diagnostic performance is controlled by an analysis of the sensitivity of the residues to uncertainties and defects. To improve diagnostic performance, determine the indices performance (sensitivity index and detectability index) [55].

5.1 Sensitivity Index (SI)

The index of parametric standardized sensitivity explained the evaluation of the energy provided by the residue uncertainty on each parameter by comparing it with the total energy provided by all uncertainties.

$$SI_n = \frac{|w_i|}{d_n} \quad (14)$$

- d_i: Uncertainty on the parameters
- i : Basic element bond graph model (*R*, *C*, *I*, *TF* and *GY)*
- w_i: Modulated entry for Uncertainty in the *parameters*

5.2 Detectability Index (DI)

The detectability index represents the difference between the efforts (or streams) provided by defects in absolute terms and that granted by all the uncertainties in absolute value.

- Junction 1

$$DI = |Y_i||e_{in}| + |Y_s| \quad d \quad (15)$$

- Junction 0

$$DI = |Y_i||f_{in}| + |Y_s| \quad d \quad (16)$$

While defects detectability conditions will be:

- The defect is not detectable: $DI \leq 0$
- The defect is detectable: $DI \rangle\ 0$

VI. MODELING AND SIMULATION RESULTS OF INCUBATOR BY BOND GRAPH MODELS

6.1 Incubator System

In this subsection, a simulation model for an incubator was developed. Modeling relies mainly on the conservation of heat and mass. The proposed model is portioned into four distinct homogeneous compartments; incubator air space, heater, wall and mattress (Figure 8).

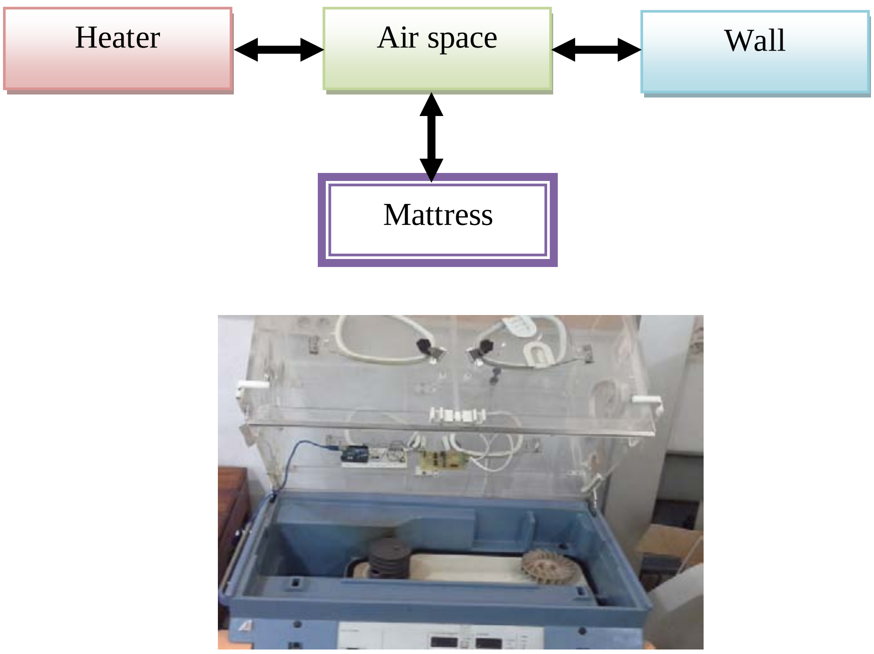

Figure 8: a) Compartments of the Closed Incubator System, b) Actual Image of the Incubator

6.2 Bond Graph Model

The incubator illustrated in figure 9 is modeled by the bond graph of figure 3 as follows:

- ★ The thermal capacity of an electrical resistor is modeled by a source of effort (Se: Te) with a capacitance (C: C_h) in series with a restriction (R_h);
- ★ The thermal capacity in the interior of the incubator by a capacitance (C: C_a) in series with a restriction (R_a);
- ★ The thermal capacity in the outside of the incubator by a capacitance (C: C_w) in series with a restriction (R_w);
- ★ The thermal capacity created by mattress by a capacitance (C: C_m) in series with a restriction (R_m);
- ★ The element (TF_1) represents the thermal transformation between the thermal source and the internal volume of the incubator.
- ★ The element (TF_2) represents the thermal transformation between the thermal source and the mattress.
- ★ The external environment is modeled by a source of effort (Se: T_{ex}) and restriction (R: Rex).

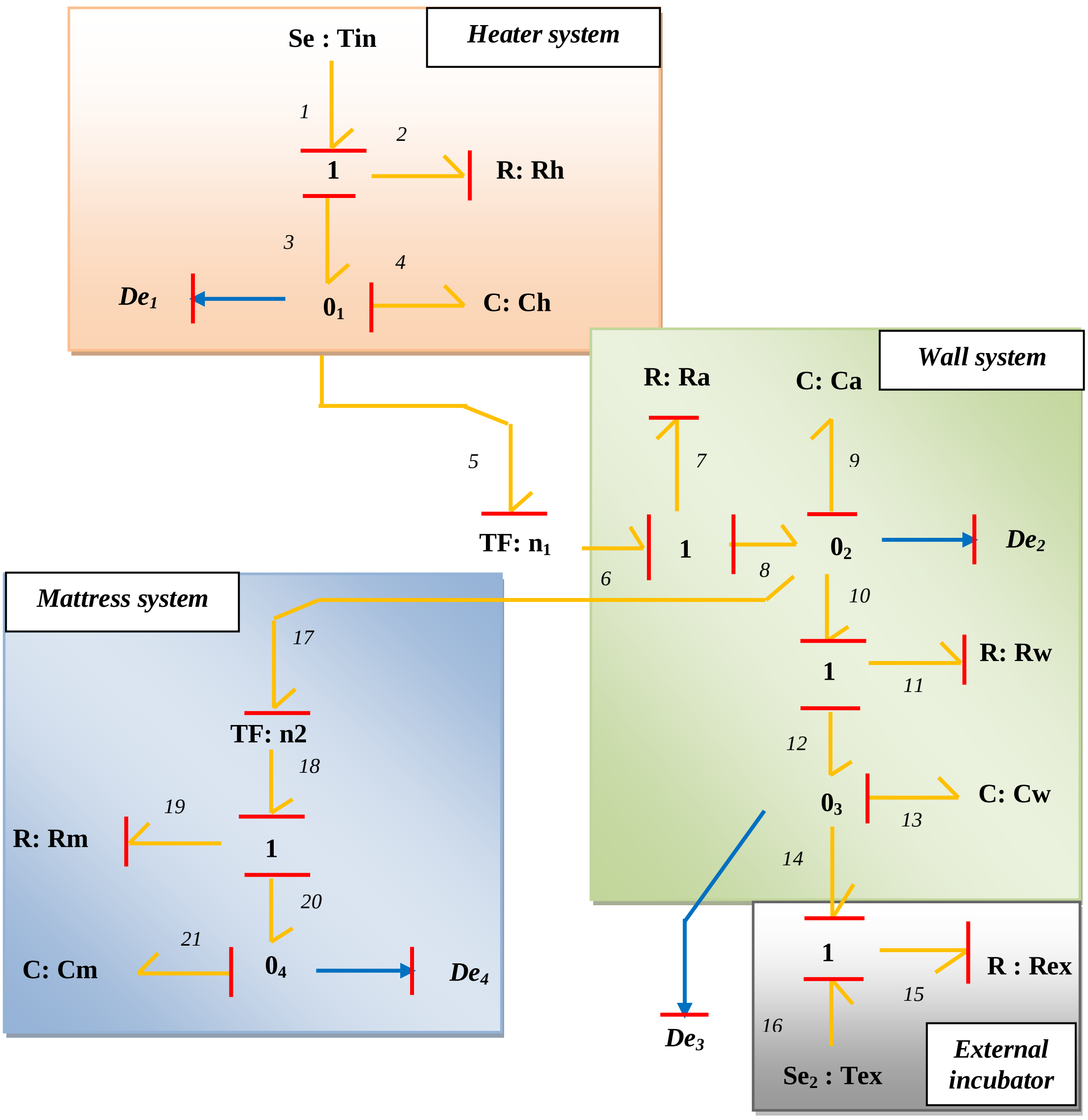

Figure 9: Bond Graph model of Incubator Technology

6. 3 Simulation Results of the Incubator

Figure 10 shows the evolution of temperature curves Th, Ta, Tw and Tm in the case of normal operation.

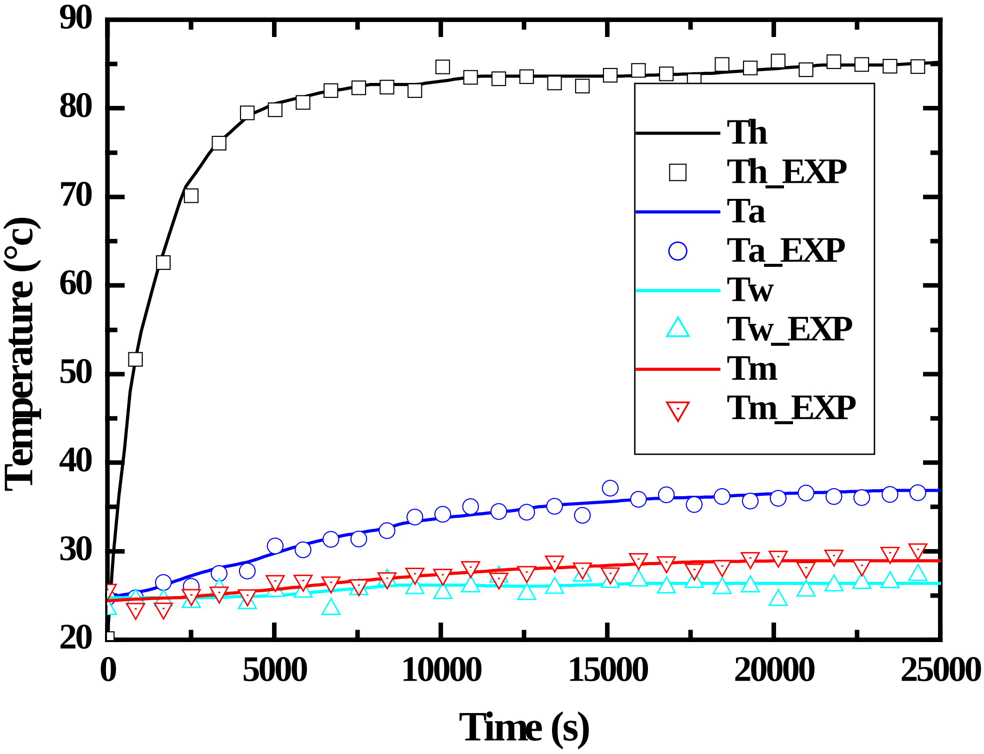

Fig. 10: Evolution of Temperature Curves Th, Ta, Tw and Tm in the Case of Normal Operation

- Determination of residue equations

❖ *The junction 0_1 gives us as equation:*

$$r_1 = f_3 - f_4 - f_5$$

According to these relations, one can deduce the residual equation r_1:

$$r_1 = \frac{T_{inp} - De_1}{Rh} - Ch.\frac{dDe_1}{dt} - \frac{n_1.(n_1.De_1 - De_2)}{Ra} \tag{17}$$

❖ *The junction 0_2 gives us as equation:*

$$r_2 = f_8 - f_9 - f_{10} - f_{17}$$

According to these relations, one can deduce the residual equation r_2:

$$r_2 = \frac{n_1.De_1 - De_2}{Ra} - Ca.\frac{dDe_2}{dt} - \frac{n_2.(n_2.De_2 - De_{''})}{Rw} - \frac{n_3.(n_3.De_2 - De_3)}{Rm} \tag{18}$$

❖ *The junction 0_3 gives us as equation:*

$r_3 = f_{12} - f_{13} - f_{14}$

According to these relations, one can deduce the residual equation r_3:

$$r_3 = \frac{De_2 - De_3}{Rw} - Cw\frac{dDe_3}{dt} - \frac{De_3 - T_{ex}}{R_{ex}} \tag{19}$$

❖ *The junction 0_4 gives us as equation:*

$$r_4 = f_{20} - f_{21}$$

According to these relations, one can deduce the residual equation r_4:

$$r_4 = \frac{n_3.(n_3.De_2 - De_4)}{Rm} - Cm\frac{dDe_4}{dt} \tag{20}$$

The default signature matrix is associated with the set of residues (r_1, r_2, ... r_n) with the elements associated with the system (F_1, F_2, ..., F_n). We denote the value M = 1 if the residual i is sensitive to this element, the opposite case M = 0, in the end we obtain the following signatures the table represented below. In our case, we have (4) four residues (17) seventeen elements.

Table 1: Fault Signatures Matrix for the Incubator

	r_1	r_2	r_3	r_4
F_1: Tin	1	0	0	0
F_2: Tex	0	0	1	0
F_3: Ch	1	0	0	0
F_4: Ca	0	1	0	0
F_5: Cw	0	0	1	0
F_6: Cm	0	0	0	1
F_7: Rh	1	0	0	0
F_8: Ra	1	1	0	0
F_9: Rw	0	0	1	0
F_{10}: Rm	0	1	0	1
F_{11}: Rp	0	0	1	0
F_{12}: n_1	1	1	0	0
F_{13}: n_2	0	1	0	1
F_{14}: De_1	1	1	0	0
F_{15}: De_2	1	1	1	1
F_{16}: De_3	0	1	1	0
F_{17}: De_4	0	1	0	1

Figure 11 shows the evolution of residues r_1, r_2, r_3 *and* r_4 as a normal function. The pitches of the residues converge towards zero under normal operating conditions.

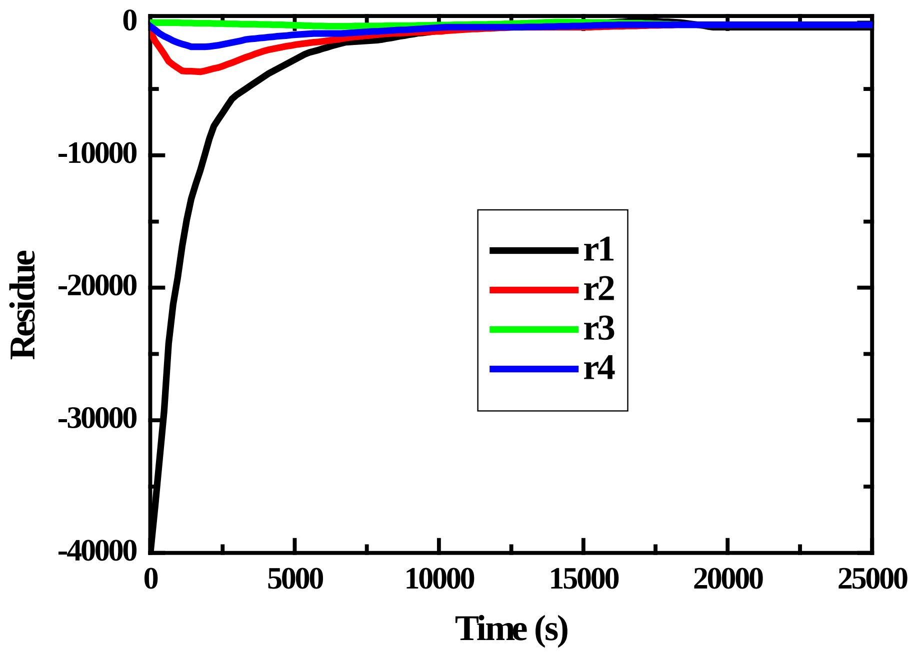

Fig. 11: Evolution of Residues r_1, r_2, r_3 *and* r_4 in the Case of Normal Operation

6. 4 Simulation Incubator With Faults

- *Fault on the Thermal Source*

When a fault occurs on the heat source (damage to the heating resistance of the incubator) at the time t = 12000s, we find that:

★ All the residues r_1, r_2, r_3 and r_4 have non-zero average values, these residues are therefore sensitive to this defect, which is confirmed, by the theoretical results presented in table 2 (see Figure 12).

★ Temperatures *Th, Ta, Tw* and Tm suffered declines in their speed at the moment of failure (see Figure 13).

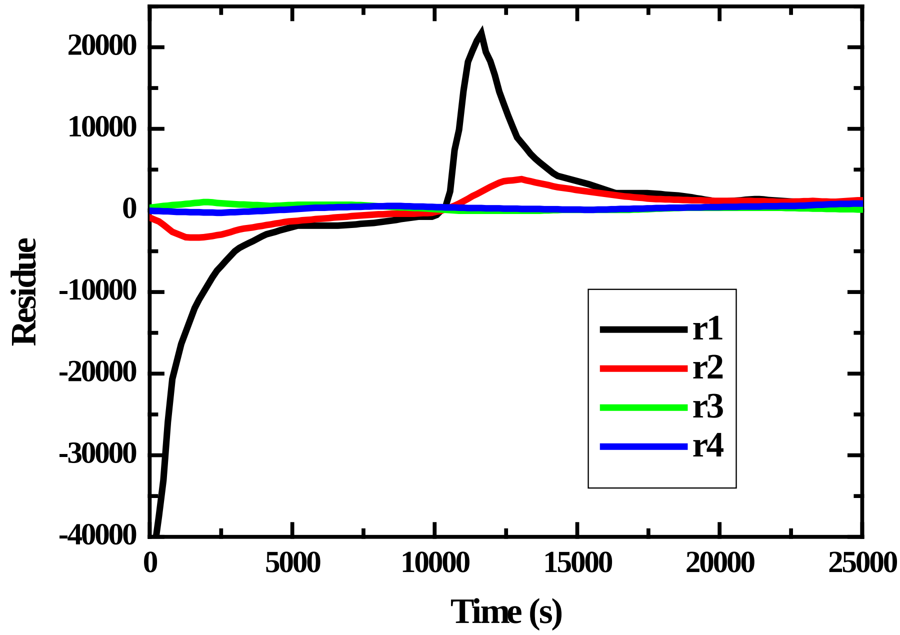

Fig. 12: Evaluation Of Residues r_1, r_2, r_3 and r_4 in the Case of a Fault on the Thermal Source

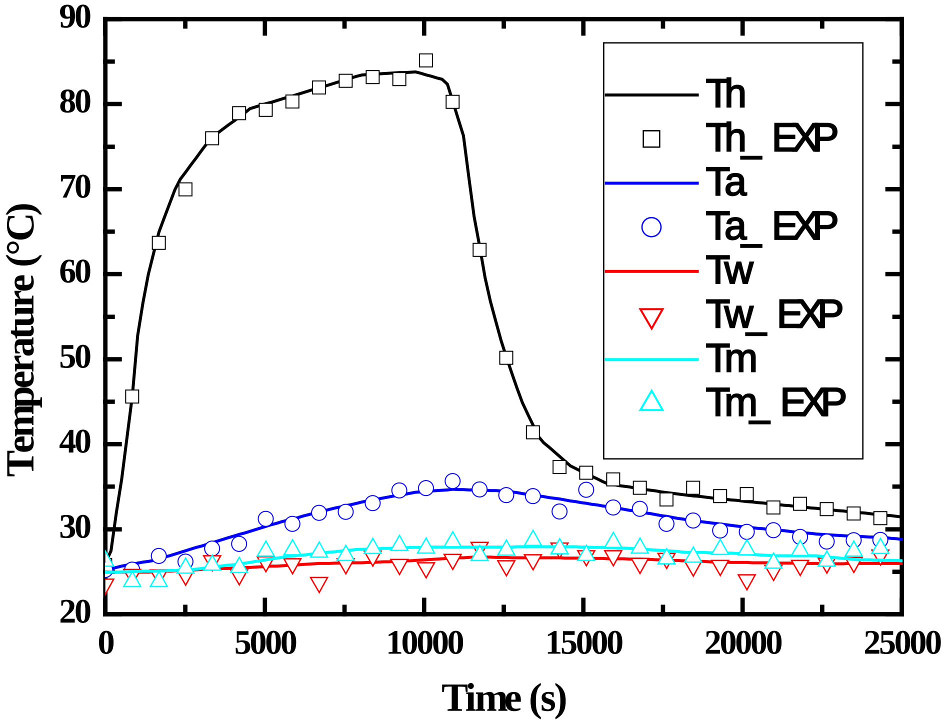

Fig. 13: Evaluation of temperatures *Th, Ta, Tw* and *Tm* in the case of a fault on the thermal source

- Fault inside the incubator

When a fault occurs on the incubator (open door of the incubator) at the time t = 17000s, we find that:

★ The residues r1, r2, r3 and r4 have non-zero average values, these residues are therefore sensitive to this defect, which is confirmed, by the theoretical results presented in table 2 (see Figure 14).

★ Temperatures Th, Ta, Tw and Tm suffered declines in their speed at the moment of failure (see Figure 15).

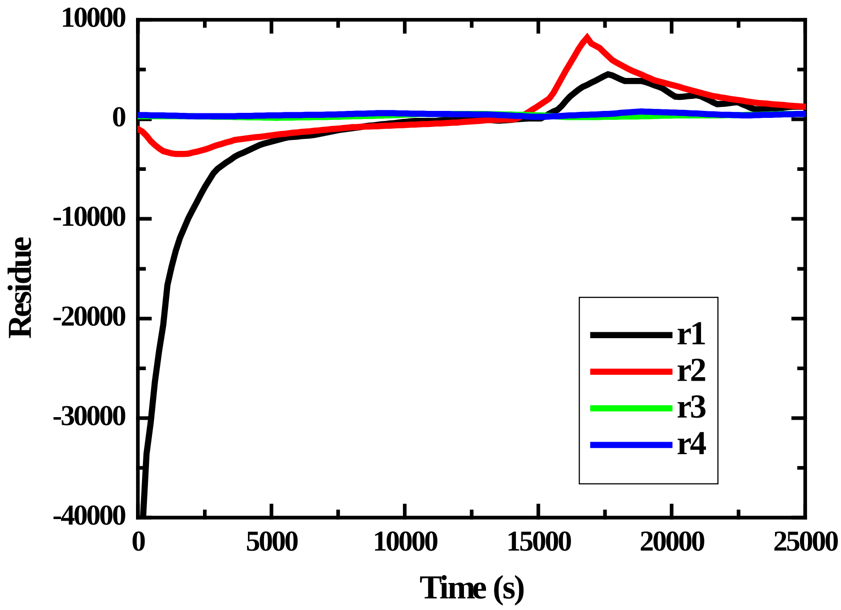

Fig. 14: Evaluation of Residues r_1, r_2, r_3 and r_4 in the Case of Default in Inside the Incubator

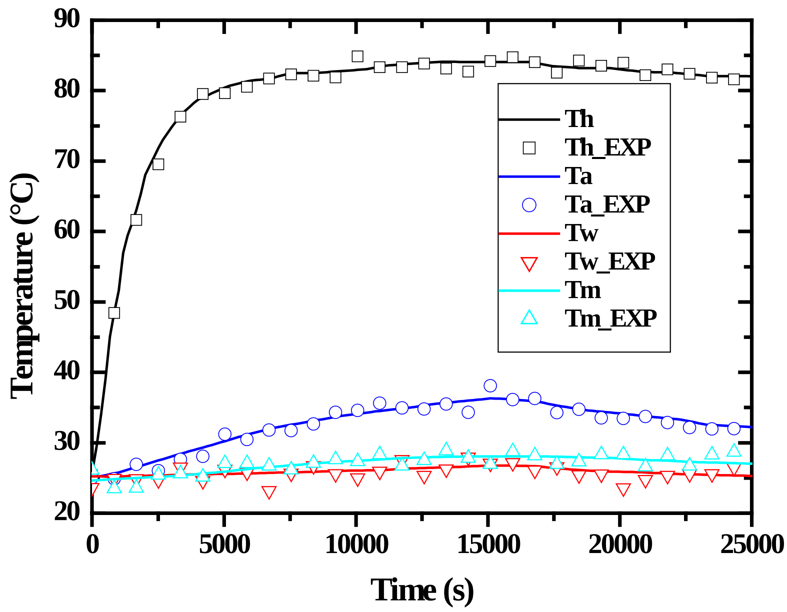

Fig. 14: Evaluation of Temperatures *Th, Ta, Tw* and *Tm* in the Case of Default in Inside the Incubator

VII. ROBUST DIAGNOSIS BY BOND GRAPHS

7.1 BG-LFT Model of the Incubator Flawless

Figure 16 shows the BG-LFT model of the incubator system flawless. To determine the residues, we must put the system in the form derivative and also put sensors under dialyzed.

- *Determination of residues flawless*

★ The junction 0_1 gives us as equation:

$$R_{d1} = f_3 - f_4 - f_5 + w_{Ch} + w_{1/Rh} + w_{1/Ra}$$

From this relation, we can deduce the residual equation Rd_1:

$$Rd_1 = \frac{T_{inp} - De_1}{Rh} - Ch.\frac{dDe_1}{dt} - \frac{n_1.(n_1.De_1 - De_2)}{Ra} + w_{Ch} + w_{\frac{1}{Rh}} + w_{\frac{1}{Ra}} \tag{21}$$

The equation consists of two parts: the first part is the normal evolution of the residual r_{1n} and the second part represents the residual uncertainty related to the evolution of the parameters d_1:

$$\begin{cases} Rd_1 = r_{1n} + d_1 \\ r_{1n} = \dfrac{T_{inp} - De_1}{Rh} - Ch.\dfrac{dDe_1}{dt} - \dfrac{n_1.(n_1.De_1 - De_2)}{Ra} \\ d_1 = w_{Ch} + w_{\frac{1}{Rh}} + w_{\frac{1}{Ra}} + w_{\frac{1}{Rw}} \end{cases}$$

★ The junction $\mathbf{o_2}$ gives us as equation:

$$Rd_2 = r_2 = f_8 - f_9 - f_{10} - f_{17} + w_{Ca} + w_{1/Ra} + w_{1/Rw}$$

From this relation, we can deduce the residual equation Rd_2:

$$Rd_2 = Ca.\frac{dDe_2}{dt} - \frac{De_1 - De_2}{Ra} - \frac{De_1 - De_3}{Rw} + w_{Ca} + w_{\frac{1}{Ra}} + w_{\frac{1}{Rw}} \tag{22}$$

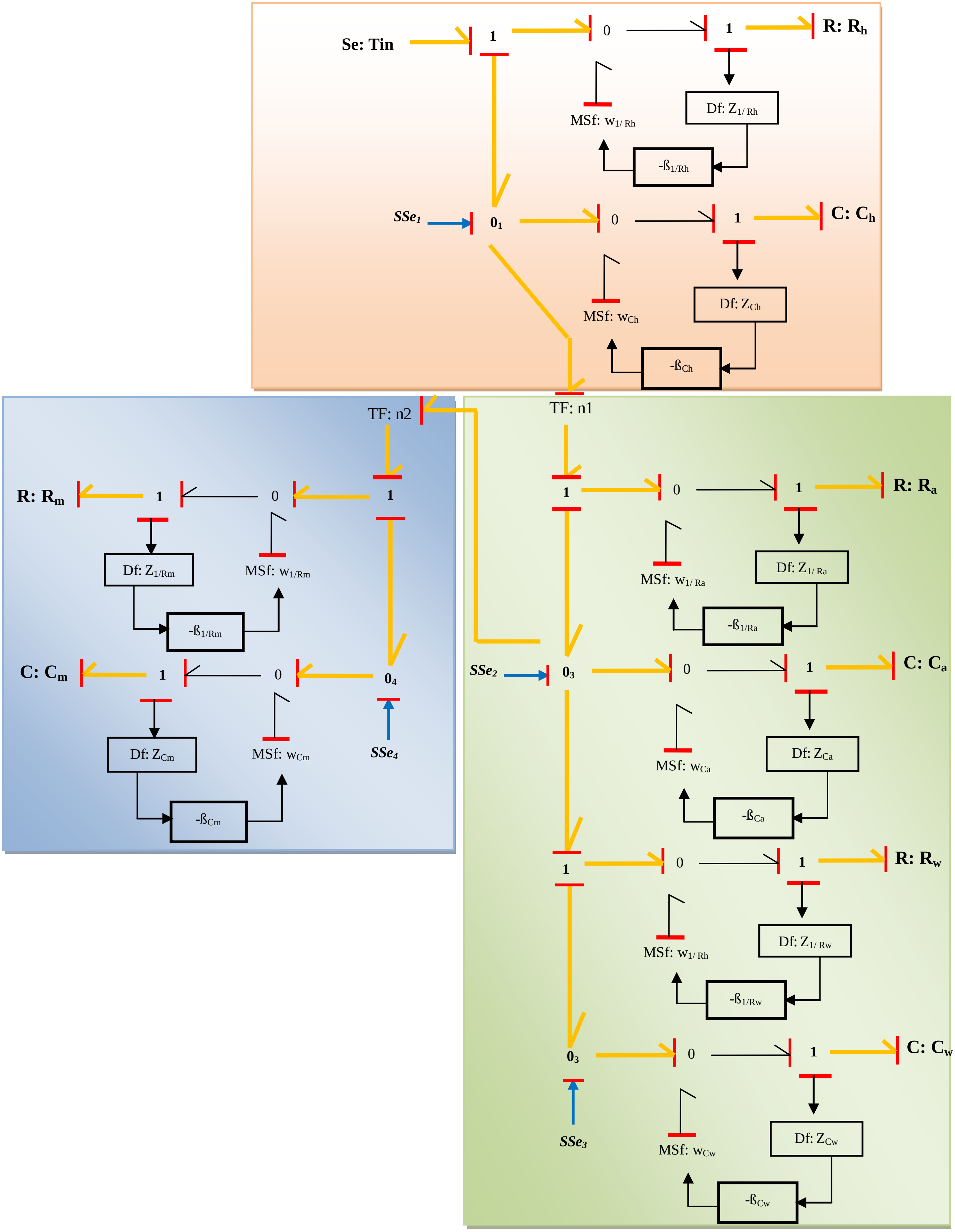

Fig. 16: GB-LFT Approach Incubator System with Derivative Mode

The equation consists of two parts: the first part is the normal evolution of the residual r_{1n} and the second part represents the residual uncertainty related to the evolution of the parameters d_1:

$$\begin{cases} Rd_1 = r_{1n} + d_1 \\ r_{1n} = \dfrac{T_{inp} - De_1}{Rh} - Ch.\dfrac{dDe_1}{dt} - \dfrac{n_1.(n_1.De_1 - De_2)}{Ra} \\ d_1 = w_{Ch} + w_{\frac{1}{Rh}} + w_{\frac{1}{Ra}} + w_{\frac{1}{Rw}} \end{cases}$$

★ The junction $\mathbf{o_2}$ gives us as equation:

$$Rd_2 = r_2 = f_8 - f_9 - f_{10} - f_{17} + w_{Ca} + w_{1/Ra} + w_{1/Rw}$$

From this relation, we can deduce the residual equation Rd_2:

$$Rd_2 = Ca.\frac{dDe_2}{dt} - \frac{De_1 - De_2}{Ra} - \frac{De_1 - De_3}{Rw} + w_{Ca} + w_{\frac{1}{Ra}} + w_{\frac{1}{Rw}} \quad (22)$$

The equation consists of two parts: the first part is the normal evolution of the residual r_{2n} and the second part represents the residual uncertainty related to the evolution of the parameters d_2:

$$\begin{cases} Rd_2 = r_{2n} + d_2 \\ r_{2n} = \dfrac{n_1.De_1 - De_2}{Ra} - Ca.\dfrac{dDe_2}{dt} - \dfrac{De_1 - De_3}{Rw} \\ - \dfrac{n_2.(n_2.De_2 - De_4)}{Rm} \\ d_2 = w_{Ca} + w_{\frac{1}{Ra}} + w_{\frac{1}{Rw}} + w_{\frac{1}{Rm}} \end{cases}$$

★ The junction $\mathbf{o_3}$ gives us as equation:

$$Rd_3 = f_{12} - f_{13} - f_{14} + w_{Cw} + w_{1/Rw} + w_{1/Rp}$$

From this relation, we can deduce the residual equation Rd_3:

$$Rd_3 = \frac{De_2 - De_3}{Rw} - Cw\frac{dDe_3}{dt} - \frac{De_3 - T_{ex}}{Rp} + w_{Cw} + w_{\frac{1}{Rw}} + w_{\frac{1}{Rp}} \quad (23)$$

The equation consists of two parts: the first part is the normal evolution of the residual r_{3n} and the second part represents the residual uncertainty related to the evolution of the parameters d_3:

$$\begin{cases} Rd_3 = r_{3n} + d_3 \\ r_{3n} = \dfrac{De_2 - De_3}{Rw} - Cw\dfrac{dDe_3}{dt} - \dfrac{De_3 - T_{ex}}{Rp} \\ d_3 = w_{Cw} + w_{\frac{1}{Rw}} + w_{\frac{1}{Rp}} \end{cases}$$

★ The junction $\mathbf{o_4}$ gives us as equation:

$$Rd_4 = f_{20} - f_{21} + w_{Cm} + w_{1/Rm}$$

According to these relations, one can deduce the residual equation Rd_4:

$$Rd_4 = \frac{n_2.(n_2.De_2 - De_4)}{Rm} - Cm\frac{dDe_4}{dt} + w_{Cm} + w_{1/Rm} \tag{24}$$

The equation consists of two parts: the first part is the normal evolution of the residual r_{4n} and the second part represents the residual uncertainty related to the evolution of the parameters d_4:

$$\begin{cases} Rd_4 = r_{4n} + d_4 \\ r_{4n} = \dfrac{n_2.(n_2.De_2 - De_4)}{Rm} - Cm\dfrac{dDe_4}{dt} \\ d_4 = w_{Cm} + w_{1/Rm} \end{cases}$$

7.2: BG-LFT Model of the Incubator with Faults

Figure 17 shows the BG-LFT model of incubator system with defaults. We have introduced seven faults, four parametric faults (Y_{Rh}, Y_{Ra},, Y_{Rw}, and Y_{Rm}) and two structural faults (Y_h *and* Y_a).

- *Determination of residues with faults*

★ The junction **0₁** gives us as equation:

$$R_{d1} = f_3 - f_4 - f_5 + w_1$$

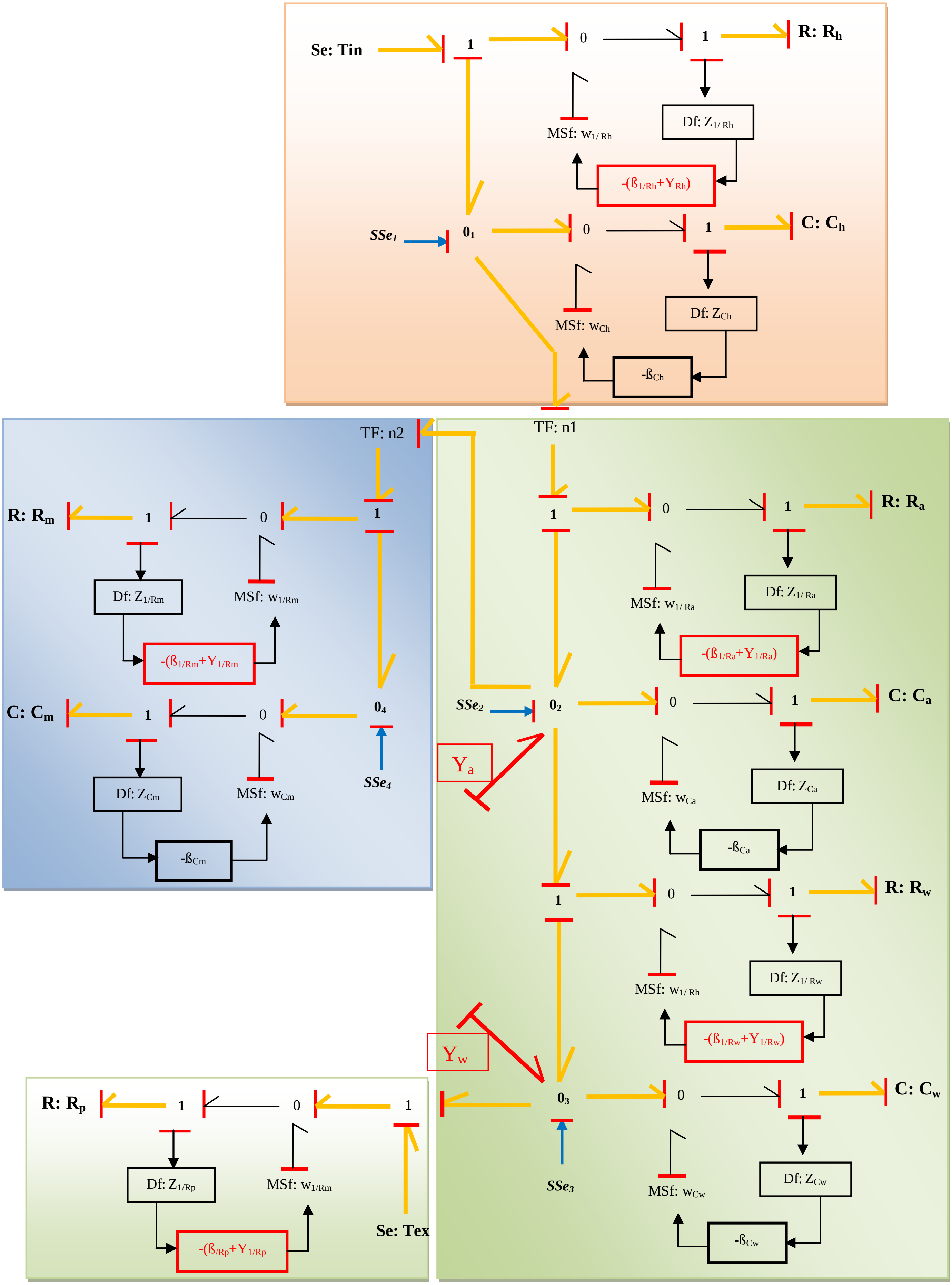

Fig. 17: BG-LFT Approach Incubator System With Derivative Mode and Four Parametric Faults (YRh, YRa,, YRw, and YRm) and Two Structural Faults (Ya and Yw)

According to these relations, one can deduce the residual equation Rd_1:

$$Rd_1 = \frac{T_{inp} - De_1}{Rh} - Ch.\frac{dDe_1}{dt} - \frac{n_1.(n_1.De_1 - De_2)}{Ra} + w_1 \tag{25}$$

With: $w_1 = w_{Ch} + w_{1/Rh} + w_{1/Ra} + Y_{1/Rh}.f_h + Y_{1/Ra}.f_a$

The equation consists of two parts: the first part is the normal evolution of the residual r_{1n} and the second part represents the residual uncertainty related to the evolution of the parameters d_1:

$$\begin{cases} Rd_1 = r_{1n} + d_1 \\ r_{1n} = \frac{T_{inp} - De_1}{Rh} - Ch.\frac{dDe_1}{dt} - \frac{n_1.(n_1.De_1 - De_2)}{Ra} \\ d_1 = w_1 \end{cases}$$

★ The junction $\mathbf{o_2}$ gives us as equation:

$$Rd_2 = f_8 - f_9 - f_{10} + w_2$$

According to these relations, one can deduce the residual equation Rd_2:

With: $w_2 = w_{1/Ra} + w_{1/Rw} + w_{Ca} + Y_{1/Ra}.f_a + Y_{1/Rw}.f_w + Y_a$

The equation consists of two parts: the first part is the normal evolution of the residual r_{2n} and the second part represents the residual uncertainty related to the evolution of the parameters d_2:

$$Rd_2 = Ca.\frac{dDe_2}{dt} - \frac{De_1 - De_2}{Ra} - \frac{De_1 - De_3}{Rw} + w_2 \tag{26}$$

$$\begin{cases} R_2 = r_{21n} + d_2 \\ r_{2n} = Ca.\frac{dDe_2}{dt} - \frac{De_1 - De_2}{Ra} - \frac{De_1 - De_3}{Rw} \\ d_2 = w_2 \end{cases}$$

★ The junction $\mathbf{o_3}$ gives us as equation:

$$Rd_3 = f_{12} - f_{13} + w_3$$

According to these relations, one can deduce the residual equation Rd_3:

$$Rd_3 = \frac{De_2 - De_3}{Rw} - Cw\frac{dDe_3}{dt} - \frac{De_3 - Tex}{Rp} + w_3 \tag{27}$$

With: $w_3 = w_{1/Rw} + w_{Cw} + Y_{1/Rw}.f_w + Y_w$

The equation consists of two parts: the first part is the normal evolution of the residual r_{3n} and the second part represents the residual uncertainty related to the evolution of the parameters d_3:

$$\begin{cases} Rd_3 = r_{3n} + d_3 \\ r_{3n} = \frac{De_2 - De_3}{Rw} - Cw\frac{dDe_3}{dt} - \frac{De_3 - Tex}{Rp} \\ d_3 = w_3 \end{cases}$$

★ The junction $\mathbf{o_4}$ gives us as equation:

$$Rd_4 = f_{20} - f_{21} + w_4$$

According to these relations, one can deduce the residual equation Rd_4:

$$Rd_4 = \frac{n_2.(n_2.De_2 - De_4)}{Rm} - Cm\frac{dDe_4}{dt} + w_4 \tag{28}$$

With: $w_3 = w_{1/Rw} + w_{Cw} + Y_{1/Rm}.f_m$

The equation consists of two parts: the first part is the normal evolution of the residual r_{4n} and the second part represents the residual uncertainty related to the evolution of the parameters d_4:

$$\begin{cases} Rd_4 = r_{4n} + d_4 \\ r_{4n} = \dfrac{De_1 - De_4}{Rm} - Cm\dfrac{dDe_4}{dt} \\ d_4 = w_4 \end{cases}$$

VIII. PERFORMANCE INDICES FOR INCUBATOR

8. 1: Sensitivity Index (SI)

Residue Rd_1:

$$\begin{cases} SI_1 = \dfrac{w_1}{d_1} \\ SI_1 = \dfrac{w_{\frac{1}{Rh}} + w_{\frac{1}{Ra}} + w_{Ch} + Y_{\frac{1}{Rh}}.f_h + Y_{\frac{1}{Ra}}.f_a}{d_1} \end{cases} \tag{29}$$

Residue Rd_2:

$$\begin{cases} SI_2 = \dfrac{w_2}{d_2} \\ SI_2 = \dfrac{w_{\frac{1}{Ra}} + w_{\frac{1}{Rw}} + w_{\frac{1}{Rm}} + w_{Ca} + Y_{\frac{1}{Ra}}.f_a + Y_{\frac{1}{Rw}}.f_w + Y_{\frac{1}{Rm}}.f_m + Y_a}{d_2} \end{cases} \tag{30}$$

Residue Rd_3:

$$\begin{cases} SI_3 = \dfrac{w_3}{d_3} \\ SI_3 = \dfrac{w_{\frac{1}{Rw}} + w_{\frac{1}{Rp}} + w_{Cw} + Y_{\frac{1}{Rw}}.f_w + Y_{\frac{1}{Rw}}.f_w + Y_w}{d_3} \end{cases} \tag{31}$$

▪ Residue Rd_4:

Residue Rd_4:

$$\begin{cases} SI_4 = \dfrac{w_4}{d_4} \\ SI_4 = \dfrac{w_{\frac{1}{Rm}} + w_{Cm} + Y_{\frac{1}{Rm}}.f_m}{d_1} \end{cases} \tag{32}$$

8.2. Detectability index (DI)

Residue Rd_1 :

In this way, the defect detectability index of the residue Rd_1 is obtained:

$$DI_1 = w_1 - d_1$$

If $DI_1 \rangle 0$ then (37)

$$\begin{cases} w_1 \rangle d_1 \\ w_{\frac{1}{Rh}} + w_{\frac{1}{Ra}} + w_{Ch} + Y_{\frac{1}{Rh}}.f_h + Y_{\frac{1}{Ra}}.f_a \rangle d_1 \end{cases}$$

- The detectable rate $Y_{1/Rh}$ of a defect on the element R_h is calculated by supposing $Y_{1/Ra} = 0$

$Y_{1/Ra} = 0$

$$Y_{\frac{1}{Rh}} \rangle \frac{d_1 - (w_{\frac{1}{Rh}} + w_{\frac{1}{Ra}} + w_{Ch})}{f_h}$$

- The detectable rate $Y_{1/Ra}$ of a defect on the element R_a is calculated by supposing $Y_{1/Rh} = 0$

$Y_{1/Rh} = 0$

$$Y_{\frac{1}{Ra}} \rangle \frac{d_1 - (w_{\frac{1}{Rh}} + w_{\frac{1}{Ra}} + w_{Ch})}{f_a}$$

Residue Rd_2 :

In this way, the defect detectability index of the residue Rd_2 is obtained:

$$DI_2 = w_2 - d_2$$

If $DI_2 \rangle 0$ then

$$\begin{cases} w_2 \rangle d_2 \\ w_{\frac{1}{Ra}} + w_{\frac{1}{Rw}} + w_{\frac{1}{Rm}} + w_{Ca} + Y_{\frac{1}{Ra}}.f_a + Y_{\frac{1}{Rw}}.f_w \\ + Y_{\frac{1}{Rm}}.f_m + Y_a.f_{Ya} \rangle d_2 \end{cases} \quad (38)$$

- The detectable rate $Y_{1/Ra}$ of a defect on the element R_a is calculated by supposing $Y_{1/Rw} = Y_{1/Rm} = Y_a = 0$

$Y_{1/Rw} = Y_{1/Rm} = Y_a = 0$

$$Y_{\frac{1}{Ra}} \rangle \frac{d_2 - (w_{\frac{1}{Ra}} + w_{\frac{1}{Rw}} + w_{\frac{1}{Rm}} + w_{Ca})}{f_a}$$

- The detectable value $Y_{1/Rw}$ of a defect on the element R_w is calculated assuming $Y_{1/Ra} = Y_{1/Rm} = Y_a = 0$

$Y_{1/Ra} = Y_{1/Rm} = Y_a = 0$

$$Y_{\frac{1}{Rw}} \rangle \frac{d_2 - (w_{\frac{1}{Ra}} + w_{\frac{1}{Rw}} + w_{\frac{1}{Rm}} + w_{Ca})}{f_w}$$

- The detectable value $Y_{1/Rm}$ of a defect on the element R_m is calculated assuming $Y_{1/Ra} = Y_{1/Rw} = Y_a = 0$

$Y_{1/Ra} = Y_{1/Rw} = Y_a = 0$

$$Y_{\frac{1}{Rm}} \rangle \frac{d_2 - (w_{\frac{1}{Ra}} + w_{\frac{1}{Rw}} + w_{\frac{1}{Rm}} + w_{Ca})}{f_m}$$

- The detectable value Y_a of the structural defect is calculated assuming $Y_{1/Ra} = Y_{1/Rw} = Y_{1/Rm} = 0$

$Y_{1/Rm} = 0$

$$Y_a \rangle \frac{d_2 - w_{\frac{1}{Ra}} + w_{\frac{1}{Rw}} + w_{\frac{1}{Rm}} + w_{Ca}}{f_{Ya}}$$

Residue Rd_3 :
In this way, the defect detectability index of the residue Rd_3 is obtained:

$$DI_3 = w_3 - d_3 \tag{34}$$

If $DI_3 \rangle 0$ then

$$\begin{cases} w_3 \rangle d_3 \\ w_{\frac{1}{Rw}} + w_{\frac{1}{Rp}} + w_{Cw} + Y_{\frac{1}{Rw}} . f_w + Y_{\frac{1}{Rp}} . f_p + Y_w . f_{Yw} \rangle d_3 \end{cases}$$

- The detectable rate $Y_{1/Rw}$ of a defect on the element R_w is calculated by supposing $Y_{1/Rp} = Y_w = 0$

$Y_{1/Rp} = Y_w = 0$

$$Y_{\frac{1}{Rw}} \rangle \frac{d_3 - (w_{\frac{1}{Rw}} + w_{\frac{1}{Rp}} + w_{Cw})}{f_w}$$

- The detectable rate $Y_{1/Rp}$ of a defect on the element R_p is calculated by supposing $Y_{1/Rw} = Y_w = 0$

$Y_{1/Rw} = Y_w = 0$

$$Y_{\frac{1}{Rp}} \rangle \frac{d_3 - (w_{\frac{1}{Rw}} + w_{\frac{1}{Rp}} + w_{Cw})}{f_p}$$

- The detectable value Y_w of the structural defect is calculated assuming $Y_{1/Rw} = 0$

$$Y_w \rangle \frac{d_3 - (w_{\frac{1}{Rw}} + w_{\frac{1}{Rp}} + w_{Cw})}{f_{Yw}}$$

Residue Rd_4 :
In this way, the defect detectability index of the residue Rd_3 is obtained:

$$DI_4 = w_4 - d_4 \tag{40}$$

If $DI_4 \rangle 0$ then

$$\begin{cases} w_4 \rangle d_4 \\ w_{\frac{1}{Rm}} + w_{Cm} + Y_{\frac{1}{Rm}} . f_m \rangle d_4 \end{cases}$$

- The detectable rate $Y_{1/Rm}$ of a defect on the element R_w is calculated by the equation:

$$Y_{\frac{1}{Rm}} \rangle \frac{d_4 - (w_{\frac{1}{Rm}} + w_{Cm})}{f_m}$$

IX. CONCLUSION

In this paper, we presented diagnostic methods using the Bond Graph approach. The analytical redundancy relationships generated using the parity space method depends on the knowledge of the degree of derivations to be applied. The advantages of using the last method are: simplicity of understanding (*ARRs*) since they correspond to relationships and variables that are displayed by the leap graph model, and then the transition to the *LFT* form made by a simple addition of modulated sources of effort and flow on the model, image of the physical process, *ARRs* are deduced directly from the graphical representation, they can be generated in symbolic form and therefore adapted to a computer implementation.

ACKNOWLEDGEMENTS

We thank the National School of Engineers of Tunis, University of Tunis El Manar to support our work.

REFERENCES

1. Valentin Gies and Thierry Soriano. *Modeling and Optimization of an Indirect Coil Gun for Launching Non-Magnetic Projectiles*. Journal Actuators, pp: 8-39, 2019.
2. Tho N.H.T. Tran, Lawrence H. Le, Vu-Hieu Nguyen, Kim-Cuong T. Nguyen, Mauricio D. Sacchi. *Sensitivity analysis of leaky Lamb modes to the thickness and material properties of cortical bone with soft tissue: A semi-analytical finite element based simulation study*. IEEE International Ultrasonics Symposium (IUS), pp: 1-4, 2015.
3. Tai Le, Hervé Colin, Franck Al Shakarchi, Tuan Tran Quoc. *Improved Matlab Simulink Two-diode Model of PV Module and Method of Fast Large-Scale PV* System Simulation. 7th International Conference on Renewable Energy Research and Applications (ICRERA). pp: 982 - 985, 2018.
4. Naima Sakami, Lahcen Boukhattem , Hassan Hamdi. *Dynamic modelisation of heat transfer between the ground and shallow basment of a villa in Marrakesh area*. International Renewable and Sustainable Energy Conference (IRSEC). pp 867 – 871, 2016.
5. M. Shaib, M. Rashid, L. Hamawy, M. Arnout, I. El Majzoub, A. J. Zaylaa. *Advanced portable preterm baby incubator*. Fourth International Conference on Advances in Biomedical Engineering (ICABME), pp 1-4,2017.
6. Rebecca Hirte, Jürgen Münch, Laura Drost. *Incubators in Multinational Corporation's development of a corporate incubator operator model*. International Conference on Engineering, Technology and Innovation (ICE/ITMC), pp : 195 – 202, 2017
7. Gamze Tilbe Sen ; Mehmet Yüksekkaya. *Desing and Test of an Incubator Analyzer*. 2018 2nd International Symposium on Multidisciplinary Studies and Innovative Technologies (ISMSIT) , pp: 1-5, 2018.
8. B. Ashish. *Temperature monitored IoT based smart incubator*. 2017 International Confere-nce on I-SMAC (IoT in Social, Mobile, Analytics and Cloud) (I-SMAC), pp: 497 – 501, 2017.
9. Muslim Ali, Murtada Abdelwahab, Sally Awadekreim, Suliman Abdalla. *Development of a Monitoring and Control System of Infant Incubator*. 2018 International Confe-rence on Computer, Control, Electrical, and Electronics Engineering (ICCCEEE), pp : 1-4, 2018.
10. Bibo Dai, Hongting Wang. *Operation Efficiency Evaluation of Science and Technology Enterprise Incubator*. 2017 10th International Symposium on Computational Intelligence and Design (ISCID), pp : 38 – 42, Volume: 2, 2017.

11. Arif Widianto, M. Raditya Gumelar, Pradipta Mahatidana, Rizky Ramadian Wijaya; Intan Nurfitri, Kresna Devara, Retno Wigajatri Purnamaningsih. *The effect of moving load on remote weight monitoring system for simple infant incubator*. 2017 International Conference on Broadband Communication, Wireless Sensors and Powering (BCWSP), pp: 1-4, 2017.
12. Dhanesh Kattipparambil Rajan, Jarmo Verho, Joose Kreutzer, Hannu Välimäki, Heimo Ihalainen, Jukka Lekkal, Mimmi Patrikoski, Susanna Miettinen. Monitoring pH, temperature and humidity in long-term stem cell culture in CO2 incubator. 2017 IEEE International Symposium on Medical Measurements and Applications (MeMeA), pp: 470 – 474, 2017.
13. Nor Asmidar, Natasha Binti, Mohd Fudzi, Nurmiza Binti. *Development of infant incubator for clinic in the rural area of Malaysia*. 2016 IEEE EMBS Conference on Biomedical Engineering and Sciences (IECBES), pp : 331'334, 2016.
14. Kubilay Tan ; Ahmet Reşit Kavsaoğlu ; Onur Koçak ; Cansu Akbay. *Remote Monitoring System For Incubator Data*. 2018 Medical Technologies National Congress (TIPT EKNO), pp : 1-4, 2018.
15. Megha Koli ; Purvi Ladge ; Bhavpriya Prasad ; Ronak Boria ; Prof. Nazahat J. Balur. *Intelligent Baby Incubator*. 2018 Second International Conference on Electronics, Communication and Aerospace Technology (ICECA), pp: 1036 – 1042, 2018.
16. B. Li, B. Liu, and A. Toguyéni. *On-the-fly Diagnosability Analysis of Labeled Petri Nets Using Minimal Explanations*. In 9th IFAC Symposium on Fault Detection, Supervision and Safety for Technical Processes - SAFEPROCESS' 2015, 2015.
17. Estrada-Vargas A.-P., Lesage J.-J et Lopez-Mellado E. *Identification of Partially Observable Discrete Event Manufacturing Systems*. IEEE 18th Conference on Emerging Technologies and Factory Automation, ETFA, Cagliari, Italy, 2013.
18. Tapia-Flores T., Lopez-Mellado E., Estrada-Vargas A.-P. et Lesage J.-J. *Petri Net Discovery of Discrete Event processes by Computing T-invariants*. IEEE 19th Conference on Emerging Technologies and Factory Automation, ETFA, Barcelona, Spain, 2014.
19. H. Leroux, D. Andreu, and K. Godary-Dejean. *Handling exceptions in petri net-based digital architecture: from formalism to implementation on fpgas*. IEEE Transactions on Industrial Informatics, 11(4):897–906, 2015.
20. H. Leroux, K. Godary-Dejean, and D. Andreu. *Complex digital system design: A methodology and its application to medical implants*. In International Workshop on Formal Methods for Industrial Critical Systems, pages 94–107. Springer, 2013.
21. B. Li, A. Toguyéni, and M. Khlif-bouassida. *On-the-fly Diagnosability Analysis of Labeled Petri Nets Using T-invariants*. In 5th International Workshop on Dependable Control of Discrete Systems - DCDS'2015, 2015.
22. Sankaranarayanan S., Sipma H. B., Manna Z., *Petri Net Analysis Using Invariant Generation*, Verification : Theory and Practice (Essays Dedicated to Zohar Manna on the Occasion of His 64th Birthday), n° 2772 in LNCS, Springer, p. 682-701, 2004.
23. Geeraerts G., Raskin J.-F., Van Begin L., *On the efficient Computation of the Minimal Coverability set of Petri nets*, ATVA '07 : Proc. of 5th Int. Symp. on Automated Technology for Verification and Analysis, vol. 4762 of LNCS, Springer, p. 98-113, 2007.
24. Ju Biao Yao, Zhu Ming Cao and Jia Tian Guo, *The Research of Hybrid Bond Graph Modeling* . IOP Conf. Series: Journal of Physics: Conf. Series 1087 (2018) 052013 doi :10.1088/1742-6596/1087/5/052013.
25. Belkacem Ould Bouamama, Ibrahim Abdalah and Anne-Lise Gehin. *Bond Graphs as Mechatronic Approach for Supervision Design of Multisource Renewable Energy System*. IOP Conference Series: Materials Science and Engineering, Volume 417, 5th International Conference on Mechanics and Mechatronics Research (ICMMR 2018)19–21 July 2018, Tokyo, Japan

26. S. Samaddar, P. Kushwaha and S. K. Ghoshal, *Bond graph modelling and simulation of a variable inertia flywheel.* IOP Conf. Series: Materials Science and Engineering 377 (2018) 012206 doi:10.1088/1757-899X/377/1/012206.
27. Borutzky W. Bond graphs for modelling, control and fault diagnosis of engineering systems. New York: Springer Science & Business Media, 2017.
28. M. Bendaoud, H.Hihi,b and K. Faitah. Structural Controllability of Switched Linear Singular Systems Modelled by Bond Graph. International Journal of Engineering Research in Africa. Vol. 38, pp 26-45, 2018.
29. Abdallah I, Gehin A-L, Bouamama BO. Functional hybrid bond graph for operating mode management. IFACPapersOnLine 2016;49:327e32.
30. Gawthrop PJ, Bevan GP. Bond-graph modeling. IEEE control Syst 2007;27:24e45.
31. Simon BN Jr, Reddy NP, Kantak A, A theoretical model of infant incubator dynamics, J Biomech Eng. 1994 Aug;116 (3):263-9.
32. Pauline Décima, Loïc Dégrugilliers, Stéphane Delanaud, Erwan Stephan, Jean-Luc Vanhée, J.-P. Libert, Conception d'un logiciel de calcul de la thermoneutralité dans les incubateurs fermés pour nouveau-nés prématurés (projet Pretherm®) April 2012 IRBM 33(2):48–54
33. Mohamed aymen Zermani, Feki Elyes, Abdelkader Mami, Building simulation model of infant-incubator system with decoupling predictive controller September 2014 IRBM 35(4)
34. Andrés Fraguela , Francisca . Matlalcuatzi , Ángel M. Ramos, Mathematical modelling of thermoregulation processes for premature infants in closed convectively heated incubators Comput Biol Med. 2015 Feb;57:159-72
35. Stéphane Delanaud, Pauline Decima, Amandine Pelletier, Jean-Pierre Libert, Estelle Durand, Erwan Stephan-Blanchard, Véronique Bach, Pierre Tourneux, Thermal management in closed incubators: New software for assessing the impact of humidity on the optimal incubator air temperature, Medical Engineering & Physics · 46 2017, 98-95.
36. J. S. Ultman, S. Berman, P. Kirlin, J.M. Vireslovic, C.B. Baer, K.H. Marks, "Electrically heated simulator for relative evaluation of alternative infant incubator environments", Med. Instrum., 1988, vol. 22(1), pp.33-8.
37. M. H. LeBlanc, "The physics of thermal exchange between infants and their environment", AAMI Technology Assessment Report, Feb. 1987. Vol. 21 (No.1), pp. 11-15.
38. Saumya Ranjan Sahoo , Shital. S. Chiddarwar. Mobile Robot Control Using Bond Graph and Flatness Based Approach. Procedia Computer Science 133 (2018) 213–221.
39. Vijay P, Samantaray A, Mukherjee A. A bond graph modelbased evaluation of a control scheme to improve the dynamic performance of a solid oxide fuel cell. Mechatronics 2009;19:489e502.
40. Vijay P, Samantaray A, Mukherjee A. Bond graph model of a solid oxide fuel cell with a c-field for mixture of two gas species. Proc Institution Mech Eng Part I J Syst Control Eng 2008;222:247e59.
41. Hassan. Javed, A. Mahmood. A Study of Thermodynamics and Bond Graph Modelling of Evaporation in Infant Incubator. Conference Paper (PDF Available) · December 2013 with 212 Reads.
42. H., Paynter, *Analysis and design of engineering systems*, (M.I.T.Press, 1961).
43. S. Ben Mabrouk ,H. Oueslati ,R. Andoulsi " Bond- Graph modelling of water evaporation in a convective solar dryer" Proc. Of The Seventh International Conference on Renewable Energies and the Environmen eds, Tunisia, pp.1-12,2013,in press.
44. D.C., Karnopp. and R.C., Rosenberg, *Systems Dynamics: a Unified Approach*, (Mac Graw Hill, 1983).
45. R.C., Rosenberg, *Introduction to physical System Dynmics*, Series in mechanical engineering, (Mac Graw Hill, 1983).
46. M., Tagina. and G., Dauphin, Tanguy, *La méthodologie bond graph. Principes et applications*, (Centre de Publication Universitaire, 2003).

47. A., Sallami, N., Zanzouri, B., OuldBouamama, Robust Supervision of Industrials Systems by Bond Graph and External Models, *International Journal of Enhanced Research in Science Technology & Engineering*, 5 (2016) 245–258.
48. A., Sallami, N., Zanzouri, K, Mekki, Robust Fault Diagnosis Observer of Dynamical Systems Modelled by Bond Graph Approach, *8th IFAC Symposium on Fault Detection, Supervision and Safety of Technical Processes (SAFEPROCESS),*12(2012), pp. 415–420.
49. M.A., Djeziri, B., OuldBouamama and R., Merzouki, *Modelling and robust FDI of steam generator using uncertain bond graph model*. J. Process Control, 19 : (2009) 149-162. DOI:10.1016/j.jprocont.(2007).12.009.
50. Z., Han, W., Li and S.L., Shah, *Fault detection and isolation in the presence of process uncertainties*. Proceedings of the 15th IFAC World Congress, (WC' 02), (2002) pp: 1887-1892.
51. D., Henry, D. and A. Zolghari, *Norm-based design of robust FDI schemes for uncertain systems under feedback control: Comparison of two approaches*. Control Eng. Pract., 14: (2006) 1081-1097. DOI: 10.1016/j.coneng-prac.
52. M.A., Djeziri, B., OuldBouamama and R., Merzouki, *Modelling and robust FDI of steam generator using uncertain bond graph model*. J. Process Control, 19 : (2009) 149-162. DOI:10.1016/j.jprocont.(2007).12.009.
53. D., Alazard, C., Cumer, P., Apkarian, M., Gauvrit and G. Fereres, *Robustesse et Commande Optimale*. 1st Edn., Cépadues-Editions, Toulouse, ISBN-10: (199) 2854 285166, pp: 348.
54. A., Oustaloup. *La robustesse*. 1st Edn., Hermès, ISBN-10: (1994) 2.86601.442.1.
55. M.A., Djeziri, *Diagnostic des systèmes incertains par l'approche bond graph*. Thèse de Doctorat, École Centrale de Lille (2007).